PREDICTION OF THE EFFECT OF PRIMARY AND SECONDARY AIR SWIRL ON THE FLOW FIELD IN A GAS TURBINE COMBUSTOR

حساب تأثير تدويم الهواء الابتدائى والثانوى على مجالات السريان فى غرفة احتراق توربين غازى

BY

Abdel Salam H. A., El-Emam S. H., and Zawia M. S. T.
Dept. of Mechanical Power Engineering,
University of Mansoura - El Mansoura – Egypt

الخلاصة: يهدف هذا البحث الى دراسة مجالات السريان وتقدير تأثير تدويم كل من الهواء الابتدائى والثانوى على خطوط السريان، السرعات المتوسطة، كمية الاضطراب وتوزيع الضغوط داخل غرفة احتراق توربين غازى. تم استخدام برنامج حاسوب (STARPIC) و تطويره لدراسة تأثير تدويم كل من الهواء الابتدائى والثانوى على مجالات السريان داخل غرفة الاحتراق. فى هذه الدراسة تم تغيير رقم التدويم للهواء الابتدائى من الصفر الى١,٢٢٤ كما تم تغيير شدة تدويم الهواء الثانوى وأمكن الحصول على أشكال لخطوط السريان، السرعات المتوسطة، طاقة الاضطراب، وتوزيع الضغوط داخل غرفة الاحتراق تحت تأثير هذه الظروف.

وتوضح النتائج التى تم التوصل اليها أن تدويم الهواء الابتدائى و الثانوى يؤثر تأثيرا كبيرا على مجالات السريان داخل غرف احتراق التوربينات الغازية، ففى حالة تدويم الهواء الابتدائى فقط تظهر منطقة إعادة دوران مركزية عند مدخل الغرفة، وتتسع هذه المنطقة مع زيادة شدة التدويم. وفى حالة تدويم الهواء الثانوى فقط فان خطوط السريان تنتشر فى الاتجاه الرأسى بدءا من موضع دخول الهواء الثانوى لغرفة الاحتراق. كما أظهرت النتائج أن منطقة إعادة الدوران المركزية تزداد اتساعا فى حالة تدويم الهواء الابتدائى والثانوى معا مما يؤدى بالتالى الى تحسن درجة خلط الوقود مع الهواء وطول زمن البقاء للمخلوط فى منطقة اللهب وهذا يعنى تحسين كفاءة الاحتراق وأيضا تقليل نسب الملوثات فى عوادم غرف احتراق التوربينات الغازية أثناء التشغيل. وبمقارنة النتائج التى تم الحصول عليها للسرعات المتوسطة عند أرقام مختلفة لتدويم الهواء الإبتدائى مع نتائج دراسات سابقة عند نفس الظروف تم الحصول على توافق جيد.

ABSTRACT

This paper aims to study the isothermal flow field in a gas turbine combustor under different swirl conditions. The main objective is to determine the effects of primary and secondary air swirl on isothermal flow field patterns, time- mean velocities, turbulence quantities, and pressure distribution in the gas turbine combustor.

Accepted August 30, 1999

A well established computer model, STARPIC, has been applied and modified to predict the individual and combined effects of primary and secondary air swirl on the flow field in the gas turbine combustor. The primary air swirl number is varied from 0.0 to 1.224 while two strengths of secondary air swirl are considered. Predictions of streamlines, velocity profiles, turbulence energy, and pressure distribution under these primary and secondary air swirl conditions have been obtained.

Results show that primary and secondary air swirl greatly affects the flow field in the gas turbine combustor. For runs with primary air swirl only, central toroidal recirculation zone appears near the inlet of the combustor, this zone becomes wider as the swirl number is increased. For runs with secondary air swirl only, the streamlines are distributed across the radial direction in the combustor starting from the point where the secondary air is introduced. In the combined primary and secondary air swirl case the recirculation zone becomes wider, suggesting that good mixing of fuel with air and increased residence time can be obtained. As a result, good combustion is realized and minimum pollutant's emission is expected, during operation. The currently predicted results of velocity profiles at different primary air swirl numbers have been compared with previous work results at the same conditions and good agreement is obtained.

NOMENCLATURE

C_1, C_2, C_D	Constants, Table 1
C,U,V	Control cell volumes for φ , u, v, (m^3)
D	Combustor diameter. (m)
G	K-generation term, (N/m^3), Eq. 4 and Table 1
I, J	Mesh points, Fig. 3
K	Turbulence kinetic energy, (N m)
L	Combustor length, (m)
P	Time mean pressure, (N/m^2)
R	Swirler radius, (m)
S	Source term, Eq. 1
SAS	Secondary air swirl, Fig. 19
SN	Primary air swirl number
u, v,w	Time mean velocities in x, r, θ Directions
X, r, θ	Axial, radial, and circumferential coordinates, Eq. 1

Greek Symbols

α	Side-wall angle (°)
Γ	Turbulent exchange coefficient
ε	Turbulence energy dissipation rate, (N/m)
φ	Swirl vane angle
ρ	Time-mean density, (kg/m^3)
σ	Prandtl-Schmidt number
μ	Effective viscosity, (N. sec/m^2)
μ_l	Viscosity laminar value
ψ	Stream function

Subscripts

in Inlet

Superscripts

* Dimensionless parameter

1. INTRODUCTION

The flow field in the gas turbine combustors is of prime importance to the performance of the gas turbine as well as flame stability and emission characteristics. The flow field pattern depends on the method of introducing both primary and secondary air to the combustor. However, in swirling flow field patterns, the in-coming air may possesses a swirl component of velocity via passage through swirl vanes, and the side wall may slope at an angle, to the main flow direction.

Methods of inducing rotation in a stream of fluid can be divided into three principles categories (i) the use of guide vanes in axial flow, (ii) tangential entry of the fluid stream into a cylindrical duct, and (iii) rotation of the mechanical devices which import swirling motion to the fluid. The first and second types are generally used in practice [1] and therefore, these two types are adapted in this study. However the third type is recently used to obtain a stable flame in a lean burn swirl burner [2].

The common feature of the swirling flow field in a gas turbine combustor is a creation of a toroidal flow reversal in the middle region of the axes, that entrains and recirculates a portion of the hot combustion products to mix with the incoming air and fuel. In addition to the possibility of a recirculation zone near the upper corner the vortices are continually refreshed by the air in- coming through holes Zones of recirculating hot gas are essential for flame stability in gas turbines and furnaces However this stability is jeopardized in the lean, premixed, combustion currently adopted to minimize emissions of oxides of nitrogen [2]

2. MODELING OF FLOW FIELD IN THE GAS TURBINE COMBUSTOR

Several multi mathematical models of the flow field in gas turbine combustor have been developed, and published, to discuss the simulation and solution problems, in terms of practical application [3 - 8] The STARPIC (swirling turbulent axisymmetric recirculating flows in practical isothermal combustor geometries) is a final developed model based on numerical solution of 2-D axisymmetric problems via the stream function velocity or primitive pressure velocity approach [7]. This model is adapted in this study in order to investigate the secondary air swirl effect on the flow field in a can type gas turbine combustor Governing equations, boundary conditions, and current modification of the STARPIC model are outlined below.

2.1 Swirling Turbulent Axisymmetric Recirculating Flows Model

The primitive pressure-velocity variable-finite difference computer code was designed to predict swirling recirculating turbulence flows in axisymmetric combustor under primary air swirl conditions only [8] The technique involves a staggered grid system for axial and radial velocities, a line relaxation procedure for efficient solution of the equations, a two- equations k - ε turbulent model, a stair step boundary representation of the expansion flow, and realistic accommodation of swirl effects. Predictions of this type allow some results to be obtained more cheaply, quickly, and correctly than possible by the almost exclusive use of experimental means

2.1.1 The Governing Equations

The turbulent Reynolds equations for conservation of mass, momentum (in x, y, and θ directions), turbulence energy (k), and turbulence dissipation rate (ε), which govern the 2-D axisymmetric, swirling flow have been considered. All transport equations are similar and contain terms for convection and diffusion (via turbulent flux terms) and the source S_ϕ of a general variable (which contains terms describing the generation and dissipation of ϕ).

Through introducing turbulent exchange coefficient and the usual turbulent diffusion-flux (stress-rate of strain type) laws, it can be shown that similarity between the differential equations and their diffusion relations allows them all to be put in the common form [4].

$$\frac{1}{r}\left[\frac{\partial}{\partial x}(\rho u r \varphi) + \frac{\partial}{\partial r}(\rho v r \phi) - \frac{\partial}{\partial x}(r\Gamma_\phi \frac{\partial \phi}{\partial x}) - \frac{\partial}{\partial r}(r\Gamma_\phi \frac{\partial \phi}{\partial r})\right] = S_\phi \quad ...(1)$$

Where ρ, Γ_ϕ, u and v are density, turbulent exchange coefficient, axial velocity, and radial velocity, respectively.

For ϕ =1, equation 1 gives continuity equity, for ϕ = u, v, and w, gives three momentum equations for velocity components, and for ϕ = k and ε, gives two turbulence quantities equations. The forms for the source term Sϕ are given in Table 1, where certain parameters are defined as follows.

$$S^{u} = \frac{\partial}{\partial x}(\mu \frac{\partial v}{\partial x}) + \frac{1}{r}\frac{\partial}{\partial r}(r\mu \frac{\partial v}{\partial x}) \quad \text{.....(2)}$$

$$S^{v} = \frac{\partial}{\partial x}\left(\mu \frac{\partial u}{\partial r}\right) + \frac{1}{r}\frac{\partial}{\partial r}\left(r\mu \frac{\partial v}{\partial r}\right) \quad \text{.....(3)}$$

$$G = \mu\left[2\left\{(\frac{\partial u}{\partial x})^2 + (\frac{\partial v}{\partial r})^2 + (\frac{v}{r})^2\right\} + (\frac{\partial u}{\partial r} + \frac{\partial v}{\partial x})^2 + \left\{r\frac{\partial}{\partial r}(w/r)\right\}^2 + \left(\frac{\partial w}{\partial x}\right)^2\right] \quad \text{.....(4)}$$

$$\mu = C_1 \rho k^2 / \varepsilon + \mu_l \quad \text{.....(5)}$$

$$\Gamma_\phi = \mu / \sigma_\phi \quad \text{.....(6)}$$

Implicit here is the use of the two- equations k- ε turbulence model [7 and 9], which is commonly used in computer codes for turbulent flow prediction [2, and 10 - 14].

The above equations do not alone specify the problem; additional information of two kinds is needed: initial and boundary conditions for all the dependent variables. The solution technique is based on the pressure-velocity approach [10]. The finite difference equations are solved on a complex mesh illustrated in Fig. 1. The different control volume C, U, and V, which are appropriate for the P, W and S locations respectively are given in Fig. 2.

These equations have to be solved for the time-mean pressure p and the velocity components u, v, and w Then the other useful designer information-like streamline plots showing breakaway and reattachment points, recirculation zone and stagnation points are easily produced. Streamline plots are obtained from dimentionless axial velocity stream function, which is given by.

$$\psi^* = \int_0^r urdr / \int_0^{d/2} urdr \quad \text{.....(7)}$$

2.2 Boundary Conditions

The stair step simulation method shown in Fig.3, is utilized, in order to retain conceptual simplicity. The flow field is covered with a non-uniform rectangular grid system. Typically the boundary of the solution domain falls half way between its immediate nearby parallel grid lines, together with information concerned with the position of the sloping side wall boundary are used to determine the flow field of interest. The boundary conditions and their values used in this study are taken from [14].

2.3 Program Modification

As mentioned before, the STARPIC computer program which is adapted here, has been primary developed to simulate the flow field in gas turbine combustor under the effect of primary air swirl only. In this study this computer program has been modified to predict also the effect of secondary air swirl on the flow field in the can type gas turbine combustor under investigation. As shown in Fig. 4, the considered combustor has an inlet pipe diameter of

80 mm, a combustor diameter of 300 mm, and combustor total length of 1000 mm, with sudden upstream expansion. Four tangential slots are located close to the upstream for introducing secondary air with certain swirl strength value, (Fig. 5).

Primary air swirl number is calculated as the ratio of the axial flux of angular and axial momenta, divided by the swirler radius [7]. Secondary air strengths are related to the inlet velocity of the introduced air through the tangential slots. Values of the secondary air velocity are considered in the computer model as a tangential component at a point near the combustor wall where its effect on the tangential velocity component of the main flow was evaluated. Also the mass flow rate of the secondary air is introduced into the stream function calculation procedure.

3. RESULTS AND DISSCUSTIONS

The modified version of the STARPIC computer code is applied to simulate the isothermal air flow in the axisymmetric gas turbine combustor, in order to determine the effect of swirl on the flow patterns. The effect of air swirl on flow field required the clarification of all the important flow parameters such as: (i) flow field streamlines, (ii) recirculation zone shape and size, (iii) axial, radial, and tangential velocity components, (iv) turbulence kinetic energy, and (v) axial and radial distribution of the static pressure. Turbulence constants that have been used in this study are taken from [8] and the operating parameters are:

1- Fluid properties (density and viscosity, 1.1211 Kg/m^3 and 1.8E-5 N. sec/m^2, respectively),

2- Boundary values (inlet velocity (u_{in}), inlet turbulent energy (k_{in}), and inlet energy dissipation rate (ε_{in}), 5 m/sec, 0.03 $(u_{in})^2$, and $(k_{in})^{1.5}$ / 0.005 R, respectively,

3- Grid numbers are 21 in the radial direction and 23 in the axial direction.

The effect of primary air swirl only on the flow field parameters has been predicted at three primary air swirl numbers (SN) of 0.0, 0.7066 and 1.224. The effect of secondary air swirl has been obtained with and without considering primary air swirl. Results of two cases of secondary air swirl strengths are predicted; low swirl at slots area of 6000 mm^2 and high swirl at slots area of 4000 mm^2. The results are classified and discussed below.

3.1 Streamline Patterns

Predicted dimensionless streamline patterns with and without primary air swirl are shown in Figure 6. This figure confirms -in general – the well - known ideas about swirl effects on axisymmetric turbulent flows. As shown in the figure, a large corner recirculation zone exists at non-swirling conditions (SN = 0.0). When a low primary air swirl is introduced (SN = 0.707) a central toroidal recirculation zone appears near the inlet while the corner recirculation zone shortens considerably. As the primary air swirl is increased further more (SN = 1.224), a wider central recirculation region is established.

The effect of secondary air swirl on the streamline patterns is shown in Figs. 7 and 8. It can be seen that, a significant effect of the secondary air swirl on the streamline patterns is obtained at both low and high swirl strengths. The streamlines are distributed across the radial direction of the combustor starting from the point where the secondary air is introduced, and the recirculation zone becomes much wider.

3.2 Velocity Profiles

Velocity profiles at different axial locations of the combustor without primary or secondary air swirls are shown in Fig. 9. One can see that at the combustor inlet near the centerline, the axial velocity is maximum, while at downstream, it decreases near the centerline and shows a negative value near the wall suggesting that a recirculation zone exists near the combustor wall.

Effect of the primary air swirl on the velocity profile is shown in Figs. 10 and 11. At low primary air swirl (Fig. 10), the axial velocity profiles change dramatically, and both radial and tangential velocity profiles are shifted towards the inlet of the combustor at the center, while at upstream there is a negative axial velocity. Further downstream, both axial and tangential velocities are minimum at the center- line and they increase towards the wall direction and become maximum near the wall. At high primary air swirl (SN = 1.224) the negative axial velocity increases as shown in Fig. 11, and the recirculation zone becomes much wider.

Effect of the secondary air swirl on the dimensionless axial, radial and tangential velocity profiles is shown in Figs. 12 –16. In general, the figures show that high secondary air swirl strength (at different axial distances) decreases the axial velocity, while the tangential velocity increases reaching its maximum value near the wall. This suggests that, operating the gas turbine combustor with high strength of secondary air swirl, the flame will move around with higher velocity, smaller diameter, and shorter length. This is in good agreement with the experimental results of [14].

3.3 Turbulence Energy Distributions

The turbulence energy distributions for the flow under different swirl conditions are plotted in Figs 17 and 18. Fig. 17 shows the dimensionless turbulence energy distributions along the flow without swirl in the direction of the combustor outlet The figure indicates that maximum turbulence energy exists near the inlet at the surface of flow. As the flow moves downstream, the turbulence energy decreases and becomes uniformly distributed in the radial direction. Also Fig. 18 illustrates the effects of primary and secondary air swirl on the turbulence energy distributions. It can be seen that the turbulence energy is uniformly distributed in the radial direction, and is zero near the wall, while the turbulence energy near the wall is maximum when the secondary air swirl is introduced.

3.4 Pressure Distributions

Figure 19 shows the pressure distributions along the axial direction of the combustor for two radial locations at different swirling conditions. Fig. 19a indicates that at non- swirling conditions the dimensionless pressure increases gradually from the combustor inlet up to the exit. Also Fig. 19a shows that, when the secondary air swirl is introduced to the combustor, the dimensionless pressure becomes uniformly distributed along the combustor. The individual and combined effect of the primary air swirl on the dimensionless pressure distribution is shown in Fig. 19b. It can be concluded from this figure that a significant increase in the dimensionless pressure is obtained at the combined swirling conditions. This suggests that higher values of burning velocities can be obtained, and as a result, good combustion is realized and minimum pollutant's emission is expected, during operation.

3.5 Comparison of the Results with Previous Work Predictions

Comparison between the currently predicted results of the velocity profiles at two primary air swirl numbers (0.707 and 1.224) and previous work results [15] has been made. The comparison shows good agreement and the curves at both swirl numbers take the same trends as shown in Fig. 20. Also, the results of the effect of the secondary air swirl on the velocity profile are in good agreement with those obtained experimentally in a gas turbine combustor of the same geometry [14]. These indicate that as the secondary air swirl strength is increased the flame is moving around with higher velocity, smaller diameter, and shorter length. This may be considered as an important rule in the design of gas turbine combustors of the type used in this study

4. CONCLUSIONS

As a result of this study, the following conclusions are drawn.

1 The flow field in the gas turbine combustor has been greatly affected by both the primary and the secondary air swirl strengths. A recirculation zone has been generated with the primary air swirl, and then its volume changes to a maximum at combined primary and secondary air swirls. Therefore, at combined swirl, good mixing of fuel with air and increased residence time can be obtained, as a result, minimum pollutant emissions is expected during the operation of the combustor.

2 The primary and secondary air swirl strengths have a great influence on the axial, radial, and tangential velocities in the gas turbine combustor of the geometry used in this study. Increasing both primary and secondary air swirl strengths cause a considerable decrease in axial velocities, an insignificant change in radial velocities, and a dramatic increase in the tangential velocities at different locations in the combustor. Also, the secondary air swirl has a significant effect on the turbulent energy and pressure distributions; this indicates that good combustion and minimum emission can be obtained in operation

REFERENCES

1. Lefebvre Arthur, H, "Gas Turbine Combustion", McGraw-Hill Book Company, New York, 1983.
2. Bradley, D, Gaskell, P H., X. J. GU, Lawes, M., and Scott M. J., " Premixed Turbulent Flame Instability and NO Formation in a Lean – Burn Swirl Burner", Combustion and Flame 115:515-538, 1998
3 Lilley, D. G., "Flow Field Computer Modeling in Practical Combustors", A Review Journal of Energy, Vol. 3, pp. 193-210, July-Aug. 1979
4. Lilley, D G., "Prospects for Computer Modeling in Ram-Jet Combustor", AIAA Paper No 80-1189, Hartford, CT, June 30- July 2, 1980.
5. Rhode, D L., Lilley, D. G. and McLaughlin, D. K., " On the prediction of Swirling Flow Fields Found in Axisymmetric Combustor Geometries", ASME Symposium on Fluid Mechanics of Combustion Systems, Held in Boulder, Collorado, June 22-24 1981.
6. Gerstein, M. (ed), "Fundamentals of Gas Turbine Combustion", NASA-CP-2087, Workshop held at NASA Lewis Research Center, Cleveland, OH, Feb. 6-7 1979.
7. Launder, B. E., and Spalding, D. B., "Mathematical Models of Turbulence", Academic Press, London, England, 1972.
8 Lilley, D. G., "Primitive Pressure-Velocity Code for the Computation of Strongly Swirling Flows", AIAA Journal, Vol. 14, pp. 749-756. June 1976.
9 Launder, B. E. and Spalding, D. B., "The Numerical Computation of Turbulent Flows", Comp. Methods in Appl. Mech. And Engg., Vol. 3, pp. 269-289, 1974.
10. Roache, P. J., "Computational Fluid Dynamics", Hermosa, Albuquerque, NM, 1972.
11. Zimont, V., Polifke, W., Bettelini, M., and Weisenstein, W., "An Efficient Computational Model for Premixed Turbulent Combustion at High Reynolds Numbers Based on a Turbulent Flame Speed Closure", Transactions of the ASME, Vol. 120, July 1988.
12. Karpov, V. L., and Lipatnikov, A. N., " A Model of Premixed Turbulent Combustion and its Validation", Archivum Combustionis, Vol. 14, No. 3- 4, pp. 125- 141, 1994.
13. Bourghi, R, "Turbulent Combustion Modeling", Progress of Energy and Combustion Science, Vol. 14, No. 1, 1988.
14. Zawia, M. S T., "Swirling Influence on Combustion and Emission Characterstics in a Gas Turbine Combustor", Ph.D. Thesis, University of Mansoura, 1998.
15. Lilley, D. G., "Swirling Flows in Combustion Geometries", NASA Contract Rep. 3369, p. 191, Feb. 1981.

Table (1) The form of the source term in the general equation for Φ (Eq 1)

Φ	S_Φ
U	$-\frac{\partial p}{\partial x}+\ldots$
V	$-\frac{\partial p}{\partial r}+\frac{\rho w^2}{r}-\frac{2\mu v}{r^2}+S'$
W	$-\frac{\rho v w}{r}+\frac{\mu}{r^2}\frac{\partial}{\partial r}(ru)$
k	$G-C_{1\varepsilon}\rho\varepsilon$
ε	$(C_1\varepsilon G-C_{2\varepsilon}\rho\varepsilon^2)/k$

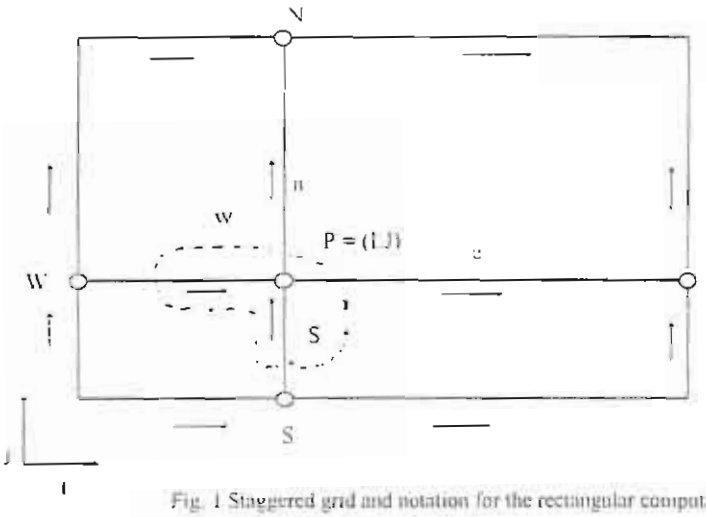

Three grids:

for P, W, etc. at position marked (O)

for velocity u - at position marked (→)

for velocity v - at position marked (↑)

Fig. 1 Staggered grid and notation for the rectangular computational mesh

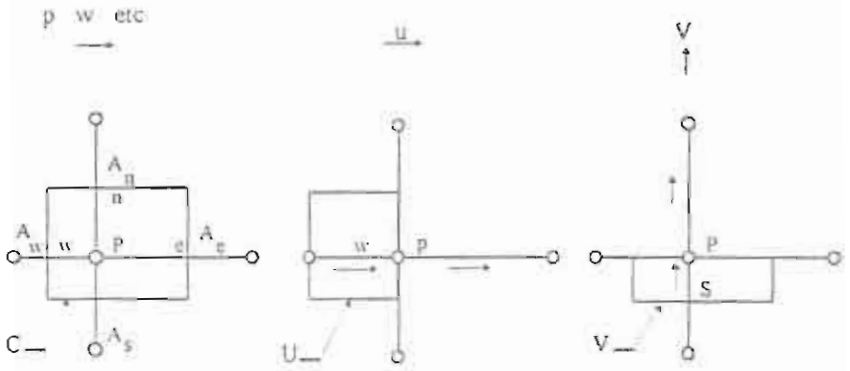

Fig. 2 The three control volumes C, U, and V associated with points of the three grids. Areas A_n, A_s, A_e and A_w for C, similar for U and V

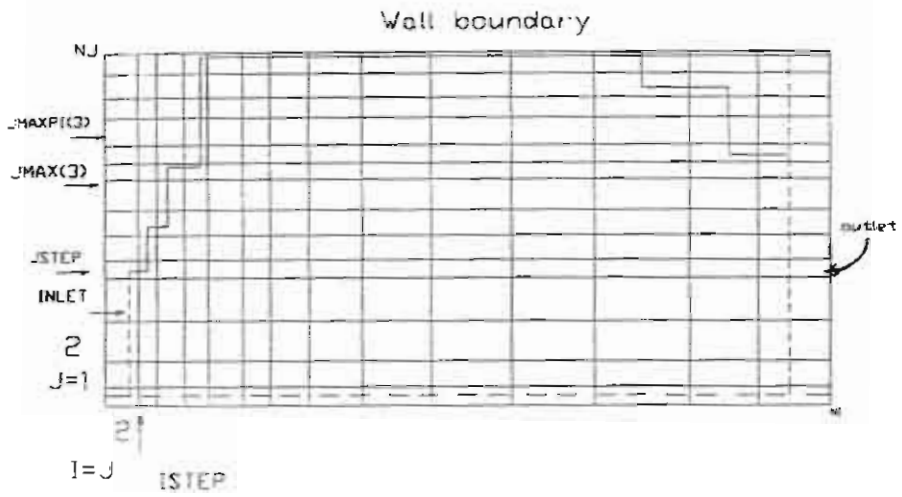

Fig. 3 Representation of grid system being employed to fit flow field domain and stair step simulation method

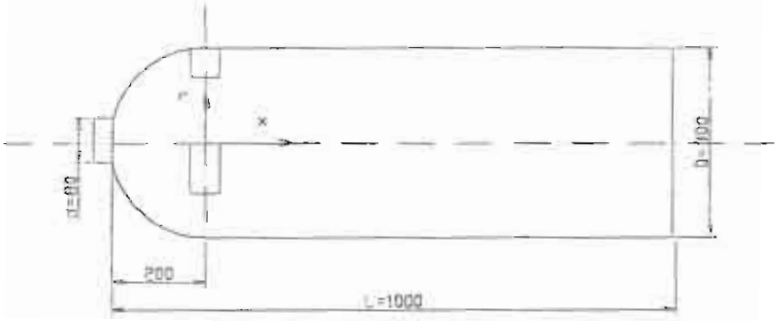

Fig. 4 Combustor model arrangement (Dimensions in mm)

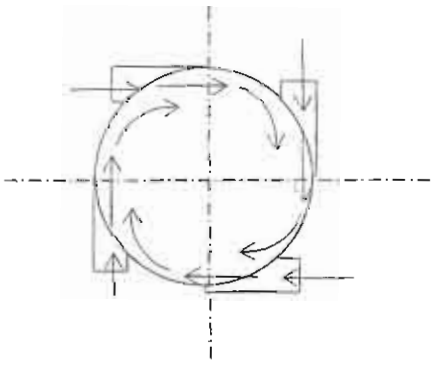

Fig. 5 Arrangement of the secondary air swirler slots.

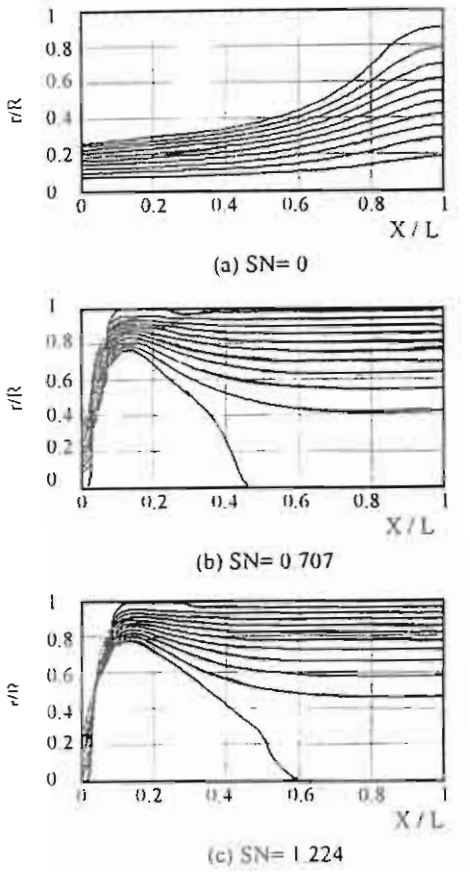

Fig. 6. Effects of primary air swirl on dimensionless streamline patterns

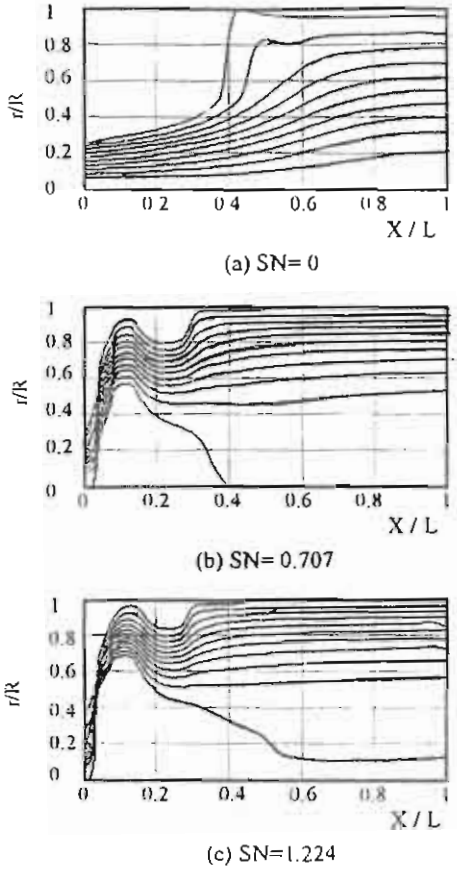

Fig . 7. Effects of low strength secondary air swirl on dimensionless streamline patterns

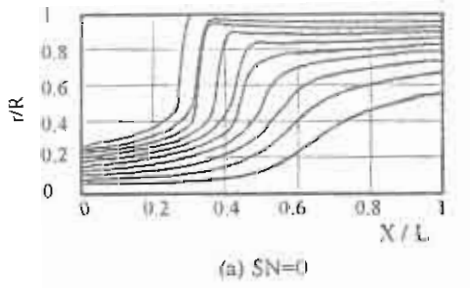

Fig. 8. Effects of high strength secondary air swirl on dimensionless streamline patterns

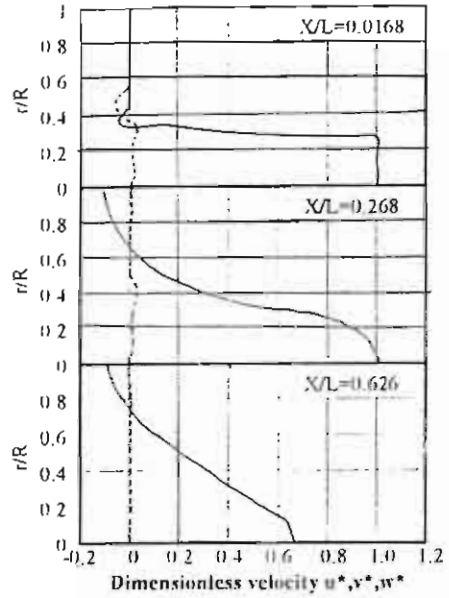

Fig. 9. Dimensionless velocity distributions along the flow direction without swirl
—— u* —— v* — — w*

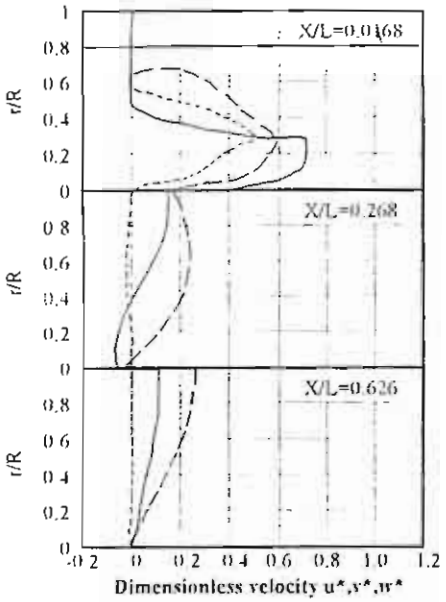

Fig. 10. Dimensionless velocity distributions along the flow direction at SN = 0.707
—— u* —— v* — — w*

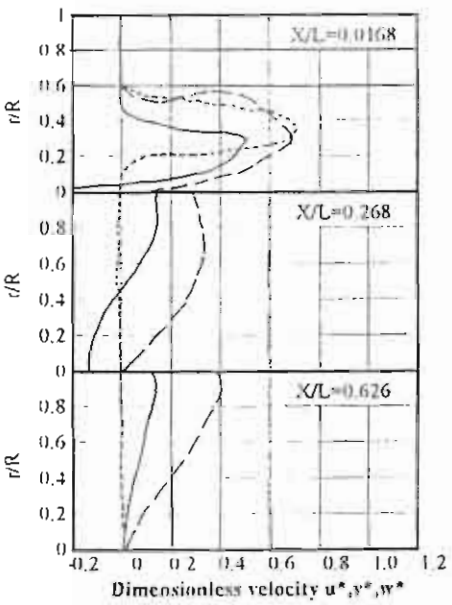

Fig. 11. Dimensionless velocity distributions along the flow direction at SN = 1.224
—— u* —— v* — — w*

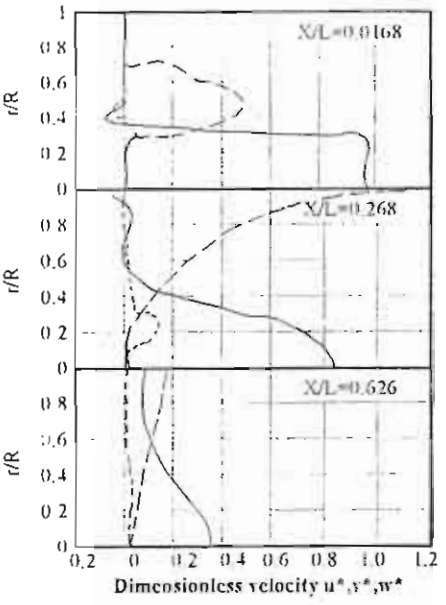

Fig. 12. Dimensionless velocity distributions along the flow direction at SN = 0 and low secondary air swirl strength
—— u* —— v* — — w*

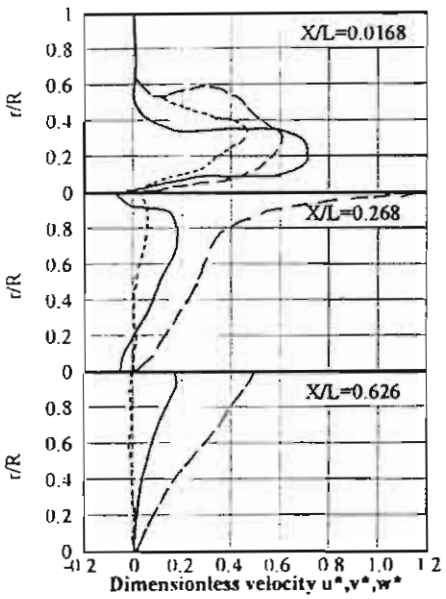

Fig. 13. Dimensionless velocity distributions along the flow direction at SN = 0.707 and low secondary air swirl strength
—— u* —— v* – – w*

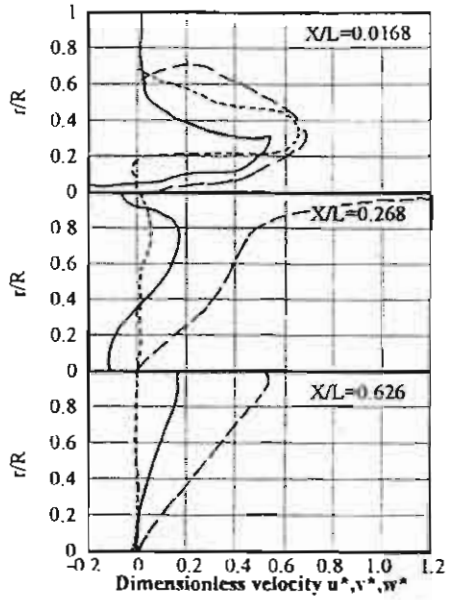

Fig. 14. Dimensionless velocity distributions along the flow direction at SN = 1.224 and low secondary air swirl strength
—— u* —— v* – – w*

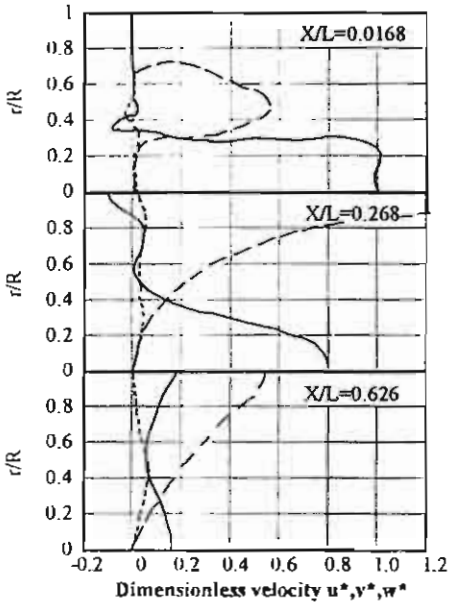

Fig. 15. Dimensionless velocity distributions Along the flow direction at SN = 0 and high secondary air swirl strength
—— u* —— v* – – w*

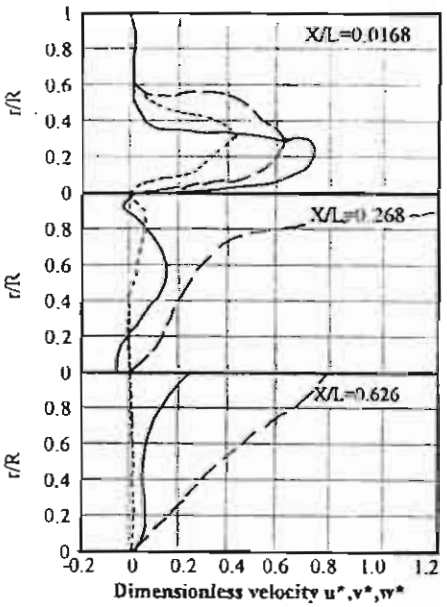

Fig. 16. Dimensionless velocity distributions along the flow direction at SN = 0.707 and high secondary air swirl strength
—— u* —— v* – – w*

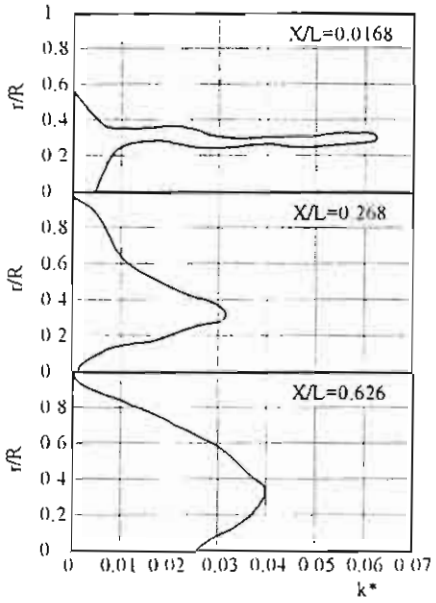

Fig. 17. dimensionless turbulence energy distributions along the flow direction without swirl

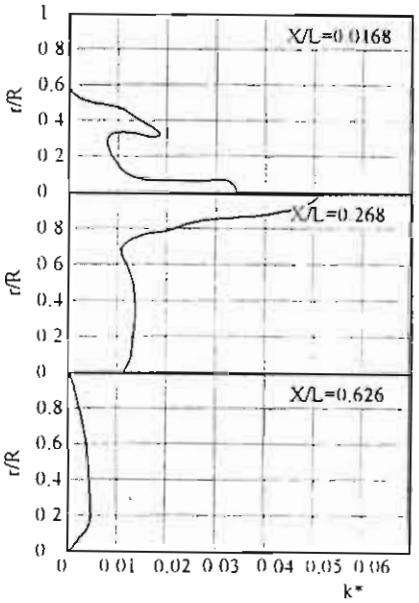

Fig. 18. Effects of secondary air swirl on turbulence energy distributions

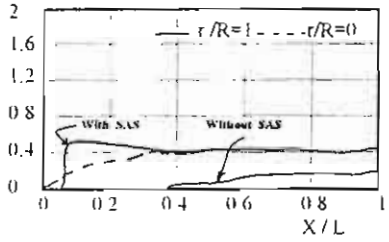

(a) SN= 0

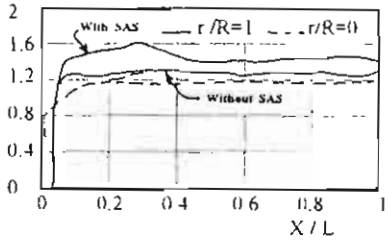

(b) SN= 0.707

Fig. 19. Effects of secondary air swirl on dimensionless pressure , p*

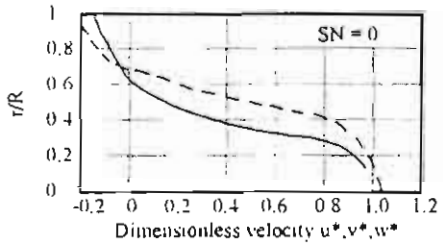

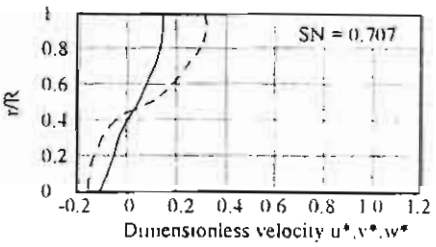

Fig. 20. Comparison between the current results for velocity profile and results from [15] at X/L=0.268
____ Current results, _ _ _ Results of [15].